Modified Transmission–Reflection Method for Measuring Constitutive Parameters of Thin Flexible High-Loss Materials

Trevor C. Williams, *Student Member, IEEE*, Maria A. Stuchly, *Fellow, IEEE*, and Paul Saville

***Abstract*—The transmission–reflection method is modified for measuring constitutive parameters of thin high-loss materials used as radar absorbers. The method uses a two-layer structure, consisting of a layer of thin flexible unknown material supported by a thicker rigid known material. The analysis and measurements focus on nonmagnetic samples of a high dielectric constant and loss factor and on the waveguide configuration in the X-band. A nonlinear least-squares optimization is used to obtain the complex permittivity from the measured scattering parameters. The uncertainty analysis presented facilitates selection of the support layer thickness. Simulations with the finite-difference time-domain method explore the effects of sample imperfections. Accuracy of a few percent can be achieved for a sample thickness of a fraction of a millimeter, provided that the thickness of the support dielectric is close to optimum and sample has only small surface imperfections.**

***Index Terms*—High-loss dielectrics, measurements, permittivity, uncertainty analysis.**

I. Introduction

VARIOUS measurement methods have been developed to evaluate the complex permittivity and permeability of materials at microwave frequencies [1]–[17]. These methods can generally be divided into the free-space and transmission-line methods. Within each of the two categories, two types of measurements can be identified, namely, broad-band and resonant techniques. Transmission-line resonant techniques have several advantages for measurements of thin samples, in particular, high sensitivity to small changes in the properties and the resultant high accuracy [1]. On the other hand, a separate resonator and sample have to be designed and fabricated for each frequency of interest. Tunable resonators tend to work only in narrow frequency ranges, they are expensive, and a decrease in the accuracy accompanies an increase in the frequency bandwidth. There are limitations of resonant methods, which are especially critical for guided-wave measurements. For free-space resonant measurements at frequencies above 10 GHz, limitations are less restrictive, and tunable resonators provide a reasonably attractive option for small frequency ranges.

The transmission–reflection (TR) method has been extensively applied and analyzed [2]–[10]. This method offers many advantages for various types of materials. However, for characterization of thin flexible materials such as radar absorbers, modification of the TR method is necessary.

In this paper, we propose a two-layer structure for measurement of radar-absorbing materials, which can only be made as thin layers. To overcome the problem of sample placement in the waveguide, the sample is deposited on a block of acrylic that fits tightly into the waveguide. The acrylic block not only maintains the sample in place, but its length can be optimized to limit the uncertainty of measurements. We present the analysis and results for an X-band waveguide, but the results apply to any waveguide or free space. This paper is organized as follows. Firstly, the relevant equations are derived relating the measured scattering parameters to the sample properties and thicknesses of the sample and acrylic. Uncertainty analysis follows to determine the optimal acrylic thickness for future measurements of the same material. While the general analysis applies to magnetic materials, the focus of this contribution is on nonmagnetic samples, as only such samples have been available for testing. Furthermore, broad-band radar absorbers can be designed using these types of materials [18]. Only limited experimental data are presented to illustrate the method feasibility, a vast database obtained for materials developed is of limited use in this paper, as the results are consistent and differ only in the permittivity values. Finally, the effect of small imperfections in the sample surface is evaluated numerically with the finite-difference time-domain (FDTD) method.

Manuscript received September 12, 2002; revised December 10, 2002. This work was supported in part by Defence Research and Development Canada Atlantic and by the Natural Sciences and Engineering Research Council of Canada under a grant.

T. C. Williams was with the Department of Electrical and Computer Engineering, University of Victoria, Victoria, BC, Canada V8P 5C2. He is now with the Department of Electrical and Computer Engineering, University of Calgary, Calgary, AB, Canada T2L 1Y3 (e-mail: willit@ucalgary.ca).

M. A. Stuchly is with the Department of Electrical and Computer Engineering, University of Victoria, Victoria, BC, Canada V8P 5C2 (e-mail: mstuchly@ece.uvic.ca).

P. Saville is with the Dockyard Laboratory Pacific, Canadian Forces Base Esquimalt, Defence Research and Development Canada Atlantic, Victoria, BC, Canada V9A 7N2 (e-mail: paul.saville@drdc.dnd.ca).

Digital Object Identifier 10.1109/TMTT.2003.810139

II. Method of Analysis and Measurements

A. Scattering Parameters for a Two-Layer Sample

The two-layer measurement configuration is shown in Fig. 1. From transmission-line theory, equations can be derived for the scattering parameters S_{11}^* and S_{21}^*.

The characteristic impedances Z_0, Z_1^*, and Z_2^* are of the empty waveguide, test sample (TS), and acrylic, respectively. Reflection coefficients Γ_1^*, Γ_2^*, and Γ_3^* are at material interfaces. The supporting acrylic layer is essentially lossless, but is kept lossy in the equations that follow to maintain their general form.

0018-9480/03$17.00 © 2003 IEEE

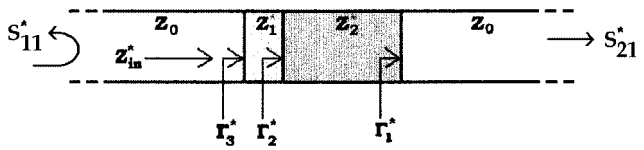

Fig. 1. Sample placement for TR measurements.

The characteristic impedances are defined in the three different media as

$$Z_0 = \frac{\sqrt{\frac{\mu_0}{\varepsilon_0}}}{\sqrt{1-\left(\frac{f_c}{f}\right)^2}}$$

$$Z_1^* = \frac{\sqrt{\frac{\mu_0}{\varepsilon_0}}\,\mu_{r1}^*}{\sqrt{\mu_{r1}^*\varepsilon_{r1}^* - \left(\frac{f_c}{f}\right)^2}}$$

$$Z_2^* = \frac{\sqrt{\frac{\mu_0}{\varepsilon_0}}\,\mu_{r2}^*}{\sqrt{\mu_{r2}^*\varepsilon_{r2}^* - \left(\frac{f_c}{f}\right)^2}} \tag{1}$$

where ε_0 is the permittivity in free space, μ_0 is the permeability in free space, ε_{r1}^* and ε_{r2}^* are the complex relative permittivities of the materials shown in Fig. 1, f_c is the cutoff frequency, and f is the frequency.

The reflection coefficients at the three interfaces indicated in Fig. 1 are

$$\Gamma_1 = \frac{Z_2 - Z_0}{Z_2 + Z_0} \quad \Gamma_2^* = \frac{Z_1^* - Z_2}{Z_1^* + Z_2} \quad \Gamma_3^* = \frac{Z_0 - Z_1^*}{Z_0 + Z_1^*}. \tag{2}$$

Rearranging (2) and expressing Γ_2^* as a combination of Γ_1 and Γ_3^* gives

$$Z_1^* = -Z_0\frac{\Gamma_3^*-1}{\Gamma_3^*+1} \quad Z_2 = -Z_0\frac{\Gamma_1+1}{\Gamma_1-1} \quad \Gamma_2^* = \frac{-(\Gamma_3^*+\Gamma_1)}{\Gamma_3^*\Gamma_1+1}. \tag{3}$$

Transmission coefficients within the two materials are

$$T_1^* = e^{-j\gamma_1^* d_1} \quad T_2^* = e^{-j\gamma_2^* d_2} \tag{4}$$

where d_1 and d_2 are the thicknesses of the respective layers and the propagation constants are

$$\gamma_1^* = \sqrt{\left(\frac{\omega}{c}\sqrt{\mu_{r1}^*\varepsilon_{r1}^*}\right)^2 - \left(\frac{\pi}{a}\right)^2}$$

$$\gamma_2^* = \sqrt{\left(\frac{\omega}{c}\sqrt{\mu_{r2}^*\varepsilon_{r2}^*}\right)^2 - \left(\frac{\pi}{a}\right)^2} \tag{5}$$

where a is the width of the waveguide.

Next, the reflection and transmission coefficients are used to calculate S_{11}^* and S_{21}^* as follows:

$$S_{11}^* = \frac{u_1^*}{v_1^*} \quad S_{21}^* = \frac{u_2^*}{v_2^*} \tag{6}$$

where

$$u_1^* = \Gamma_3^*\left(1-T_2^{*2}\right)\cdot\left(\Gamma_1^2 - T_1^{*2}\right) + \Gamma_1\left(1-\Gamma_3^{*2}T_2^{*2}\right)\cdot\left(1-T_1^{*2}\right) \tag{7}$$

$$u_2^* = T_1^*T_2^*\left(1-\Gamma_1^2\right)\cdot\left(1-\Gamma_3^{*2}\right) \tag{8}$$

$$v_1^* = v_2^* = \Gamma_1\Gamma_3^*\left(1-T_2^{*2}\right)\cdot\left(1-T_1^{*2}\right) + \left(1-\Gamma_3^{*2}T_2^{*2}\right)\cdot\left(1-\Gamma_1^2T_1^{*2}\right). \tag{9}$$

Equations (6)–(9) relate S_{11}^* and S_{21}^* to the material constitutive parameters and thicknesses for a waveguide operating in the fundamental mode. As the acrylic has known dielectric constant and thickness, S_{11}^* and S_{21}^* are functions of ε_{r1}^*, μ_{r1}^*, and d_1. Since the equations associated with the two-layer method are more complicated than for the single layer, an explicit solution for the complex permittivity ε_{r1}^* and the complex permeability μ_{r1}^* is not feasible. Even in the case of nonmagnetic materials ($\mu_{r1}^* = \mu_0$), the explicit solution cannot be easily obtained. It has been shown that optimization provides several advantages compared with an explicit solution for a single-layer TR measurement [4]. Thus, optimization is applied to solve the equations in (6)–(9). Two fourth-order polynomials represent the dielectric constant and loss factor across the frequency range of interest. The unknown coefficients of these polynomials are obtained using the constrained optimization routine *lsqnonlin* in MatLab (The MathWorks Inc., Natick, MA).

B. Uncertainty Analysis

In a classical single-layer TR method, several factors contribute to the uncertainty in the permittivity and permeability measured in a waveguide [4], namely: 1) uncertainty in the magnitude and phase of the scattering coefficients measured by a vector network analyzer (VNA); 2) errors in the sample length; 3) uncertainty in positions of the reference planes; 4) guide losses and conductor mismatch; 5) imperfect calibration due to drift in time and cable flex; 6) gaps between the sample and guide walls; and 7) higher order modes.

The latter four uncertainties are very difficult to analyze rigorously, and typically, are only estimated [4]. In the case of the two-layer TR method, additionally the acrylic thickness, its permittivity, and gaps between the guide walls contribute to the uncertainty.

Care can be taken to limit the uncertainties due to sample position, calibration, guide imperfections, higher order modes, and acrylic parameters. The main contributors to uncertainty, in addition to the uncertainty associated with the VNA, are then sample thickness and gaps between the sample and guide walls, as well as other sample imperfections. The uncertainty due to

the scattering parameters can be expressed in the general form as [4]

$$\frac{\Delta\varepsilon_{r1}^{\circ}}{\varepsilon_{r1}^{\circ}} = \frac{1}{\varepsilon_{r1}^{\circ}} \cdot \sqrt{\left(\frac{\partial\varepsilon_{r1}^{\circ}}{\partial|S_{\alpha}|} \cdot \Delta|S_{\alpha}|\right)^2 + \left(\frac{\partial\varepsilon_{r1}^{\circ}}{\partial\theta_{\alpha}} \cdot \Delta\theta_{\alpha}\right)^2} \tag{10}$$

$$\frac{\Delta\mu_{r1}^{\circ}}{\mu_{r1}^{\circ}} = \frac{1}{\mu_{r1}^{\circ}} \cdot \sqrt{\left(\frac{\partial\mu_{r1}^{\circ}}{\partial|S_{\alpha}|} \cdot \Delta|S_{\alpha}|\right)^2 + \left(\frac{\partial\mu_{r1}^{\circ}}{\partial\theta_{\alpha}} \cdot \Delta\theta_{\alpha}\right)^2} \tag{11}$$

where $\alpha = 11$ or 21, $^{\circ}$ stands for prime ($'$) or double prime ($''$), $\Delta\theta_{\alpha}$ is the uncertainty in the phase of the scattering parameters, and $\Delta|S_{\alpha}|$ is the uncertainty of the magnitude of the scattering parameter. Data $\Delta\theta$ and $\Delta|S_{\alpha}|$ are provided in the system specifications of the HP 8720C VNA. An abbreviated derivation for uncertainty of ε_r° due to the S_{21}^{*} measurement proceeds as follows.

It can be noticed that

$$\frac{\partial\varepsilon_{r1}^{\circ}}{\partial\theta_{21}} = j|S_{21}|\,\frac{\partial\varepsilon_{r1}^{\circ}}{\partial|S_{21}|} \tag{12}$$

and

$$\frac{\partial\varepsilon_{r1}^{\circ}}{\partial|S_{21}|} = \frac{\partial\varepsilon_{r1}^{\circ}}{\partial S_{21}}\,e^{j\theta_{21}} \tag{13}$$

$$\frac{\partial S_{21}}{\partial\varepsilon_{r1}^{\circ}} = \underset{15}{\frac{\partial S_{21}}{\partial\Gamma_1^{*}}}\,\underset{17}{\frac{\partial\Gamma_1^{*}}{\partial\varepsilon_{r1}^{\circ}}} + \underset{16}{\frac{\partial S_{21}}{\partial T_1^{*}}}\,\underset{18}{\frac{\partial T_1^{*}}{\partial\varepsilon_{r1}^{\circ}}} \tag{14}$$

from (6)–(9)

$$\begin{aligned}\frac{\partial S_{21}}{\partial\Gamma_1^{*}} = \frac{1}{v_2^{*}}\big[&-2\Gamma_1^{*}T_1^{*}T_2^{*}\left(1-\Gamma_3^{*2}\right)\\ &- S_{21}\left(\Gamma_3^{*}\left(1-T_1^{*2}\right)\cdot\left(1-T_2^{*2}\right)\right.\\ &\left.-2\Gamma_1^{*}T_1^{*2}\left(1-\Gamma_3^{*2}T_2^{*2}\right)\right)\big]\end{aligned} \tag{15}$$

$$\begin{aligned}\frac{\partial S_{21}}{\partial T_1^{*}} = \frac{1}{v_2^{*}}\big[&T_2^{*}\left(1-\Gamma_1^{*2}\right)\cdot\left(1-\Gamma_3^{*2}\right)\\ &- S_{21}\left(-2T_1^{*}\Gamma_1^{*}\Gamma_3^{*}\left(1-T_2^{*2}\right)\right.\\ &\left.-2\Gamma_1^{*2}T_1^{*}\left(1-\Gamma_3^{*2}T_2^{*2}\right)\right)\big]\end{aligned} \tag{16}$$

$$\frac{\partial\Gamma_1^{*}}{\partial\varepsilon_{r1}^{\circ}} = -\frac{Z_0 Z_1^{*3}}{\left(Z_1^{*}+Z_0\right)^2\eta_0^2\mu_{r1}^{*}} \tag{17}$$

$$\frac{\partial T_1^{*}}{\partial\varepsilon_{r1}^{\circ}} = -jd_1T_1^{*}\left(\frac{k_0Z_1^{*}}{2\eta_0}\right) \tag{18}$$

where k_0 is the wavenumber in free space, and η_0 is the free-space impedance $\sim$377 Ω. The equations for uncertainty resulting from S_{11}^{*} are analogous.

These expressions for uncertainty facilitate selection of acrylic thickness that results in the smallest uncertainties for given parameters of the measured sample. For example, if a material is being fabricated for measurement with approximate electrical properties, using (10), an intelligent decision can be made concerning the thickness of the supporting layer to minimize measurement uncertainty. Once this sample is measured, and a closer approximation of its electrical properties determined, (10) can be used once again to determine if a better supporting layer thickness would facilitate an even more accurate measurement.

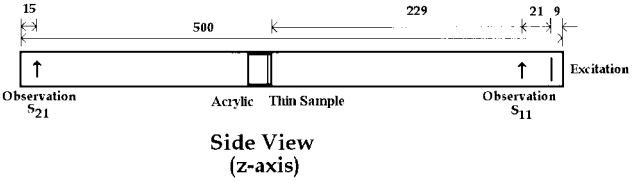

Fig. 2. FDTD simulation of the measurement setup. All dimensions are in millimeters.

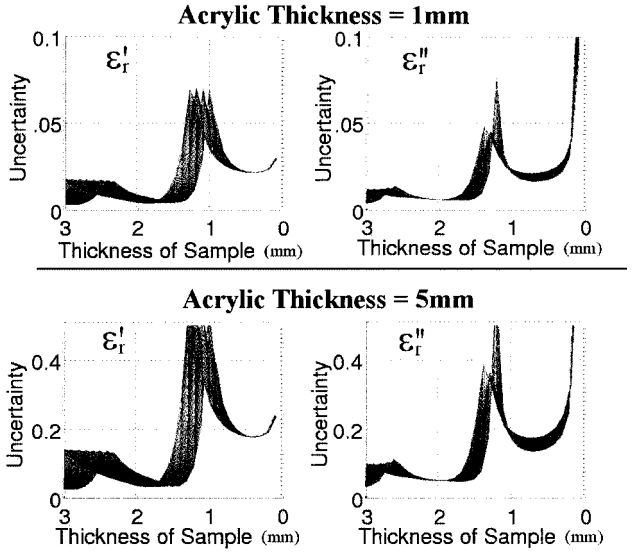

Fig. 3. Relative uncertainty ($\Delta\varepsilon'/\varepsilon'$ or $\Delta\varepsilon''/\varepsilon''$, as marked) for a TS of $\varepsilon_r' = 80$, $\varepsilon_r'' = 10$, and two acrylic thicknesses of 1 and 5 mm.

C. Uncertainty Due to Sample Gaps and Other Imperfections

Sample imperfections, such as air gaps between the sample and waveguide wall, and small dents, cannot be evaluated analytically for the two-layer configuration. These imperfections can practically be eliminated for the support material, but not for the TSs.

Simulating the actual measurement setup, a FDTD method was used to evaluate the effect of various sample imperfections. The following features were used in the simulation shown in Fig. 2:

1) fundamental (TE_{10}) waveguide mode excited with five-point sinusoidal soft source excitation across the waveguide with a frequency shifted Gaussian pulse centered on 10 GHz;
2) perfectly matched layers (nine layers, parabolic, -60 dB) applied to open ends of waveguide;
3) graded mesh (a maximum step of 1.12) used to accommodate thin layers;

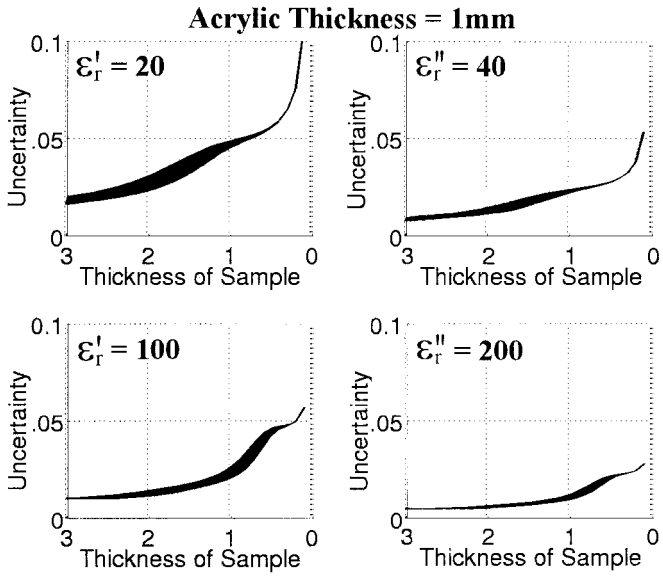

Fig. 4. Relative uncertainty ($\Delta\varepsilon'/\varepsilon'$ or $\Delta\varepsilon''/\varepsilon''$, as marked) of two sample materials.

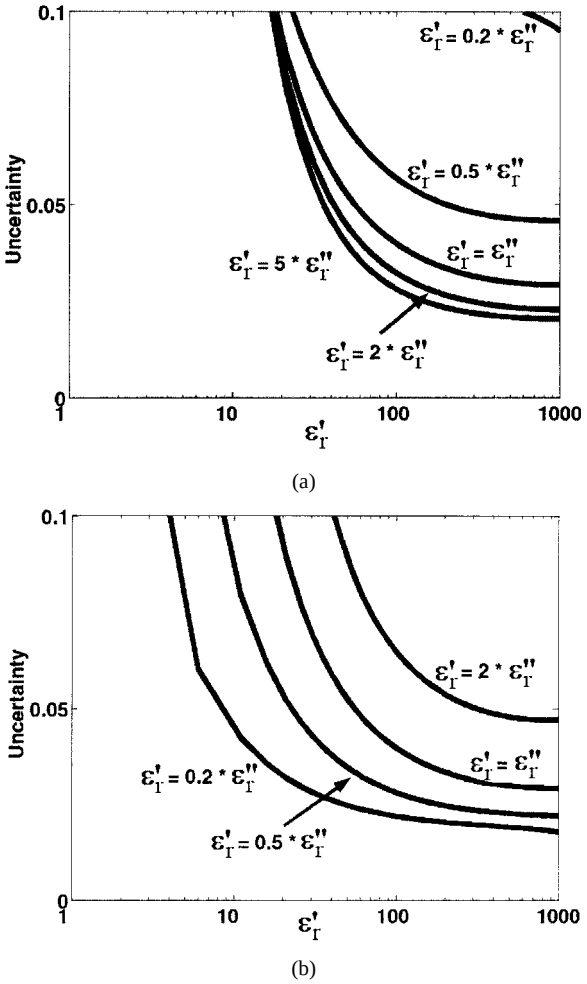

(a)

(b)

Fig. 5. Relative uncertainty: (a) $\Delta\varepsilon'/\varepsilon'$, and (b) $\Delta\varepsilon''/\varepsilon''$ for a sample thickness of 0.1 mm and acrylic thickness of 1 mm.

4) incident, reflected, and transmitted wave probe placements sufficiently removed from the sample interfaces.

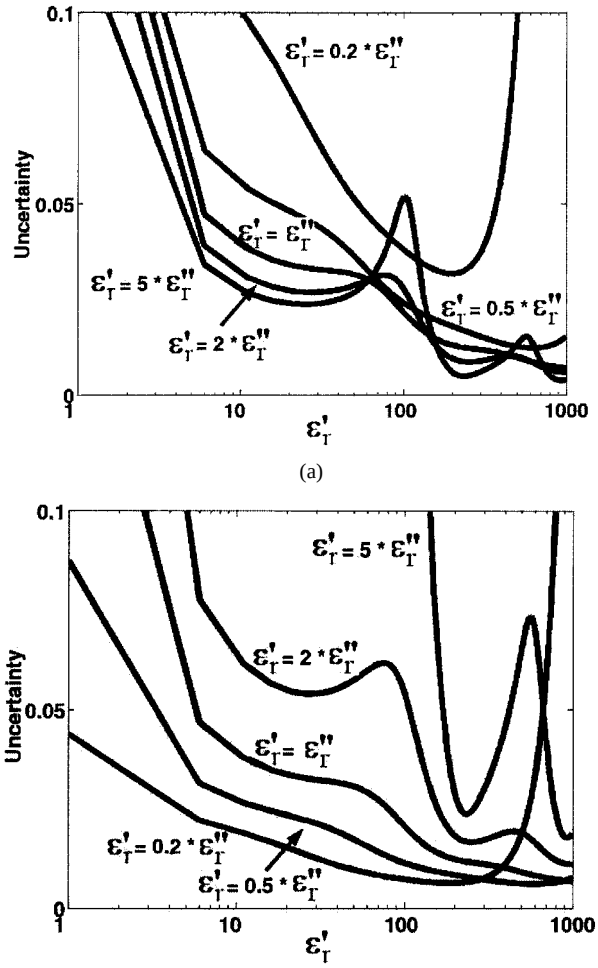

(a)

(b)

Fig. 6. Relative uncertainty: (a) $\Delta\varepsilon'/\varepsilon'$ and (b) $\Delta\varepsilon''/\varepsilon''$ for sample thickness of 1.0 mm and acrylic thickness of 1 mm.

Calibration simulations are run without the sample placed inside to facilitate collection of both S_{11}^* and S_{21}^* that resembles data collected from the VNA.

D. Measurement Procedure

Samples are provided from a chemistry laboratory researching radar absorbers. The TSs of unknown permittivity are grown directly on the acrylic as a thin layer. All measurements have been performed with a VNA HP 8720C (Agilent Technologies, Palo Alto, CA) in the X-band waveguide of width 2.286 cm and cutoff frequency f_c equal to 6.65 GHz. A standard VNA two-port calibration, 1% smoothing, and wide gating have been used. Data are collected at 401 frequency points evenly spaced from 8.2 to 12.4 GHz. Sample thickness has been of an order of 0.1–3 mm, although more typically between 0.1–0.5 mm. Typical values of the relative dielectric constant of the materials tested range from 10 to 500, and loss factor ranges from 10 to 1000. All samples are nonmagnetic ($\mu_r' = 1$, $\mu_r'' = 0$).

III. Results

The thicknesses of the sample backing acrylic and sample permittivity have a significant effect on the uncertainty of

TABLE I
RANGES OF MATERIAL PROPERTIES OVER WHICH A SPECIFIC UNCERTAINTY CAN BE MAINTAINED. SAMPLE THICKNESS = 0.1 mm

Ratio Coeff. X ($\varepsilon'_r = X\varepsilon''_r$)	Uncertainty of ε'_r				Uncertainty of ε''_r			
	< 5%		< 10%		< 5%		< 10%	
0.2	N/A	N/A	N/A	N/A	ε'_r>9.0	ε''_r>45	ε'_r>4.0	ε''_r>20
0.5	ε'_r>200	ε''_r>400	ε'_r>22	ε''_r>44	ε'_r>22	ε''_r>44	ε'_r>8.5	ε''_r>17
1	ε'_r>54	ε''_r>54	ε'_r>29	ε''_r>29	ε'_r>54	ε''_r>54	ε'_r>29	ε''_r>29
2	ε'_r>38	ε''_r>19	ε'_r>28	ε''_r>14	ε'_r>300	ε''_r>150	ε'_r>51	ε''_r>26
5	ε'_r>32	ε''_r>6.4	ε'_r>28	ε''_r>5.6	N/A	N/A	N/A	N/A

TABLE II
RANGES OF MATERIAL PROPERTIES OVER WHICH A SPECIFIC UNCERTAINTY CAN BE MAINTAINED. SAMPLE THICKNESS = 1.0 mm

Ratio Coeff. X ($\varepsilon'_r = X\varepsilon''_r$)	Uncertainty of ε'_r				Uncertainty of ε''_r			
	< 5%		< 10%		< 5%		< 10%	
0.2	ε'_r>52	ε''_r>260	ε'_r>10	ε''_r>50	ε'_r>1	ε''_r>5	ε'_r>1	ε''_r>5
0.5	ε'_r>18	ε''_r>36	ε'_r>3.4	ε''_r>6.8	ε'_r>3.4	ε''_r>6.8	ε'_r>1	ε''_r>2
1	ε'_r>6.3	ε''_r>6.3	ε'_r>3	ε''_r>3	ε'_r>6.3	ε''_r>6.3	ε'_r>3	ε''_r>3
2	ε'_r>5	ε''_r>2.5	ε'_r>2.1	ε''_r>1.1	ε'_r>120	ε''_r>60	ε'_r>4.4	ε''_r>2.2
5	ε'_r>4.4	ε''_r>.88	ε'_r>1.4	ε''_r>.08	ε'_r>190	ε''_r>38	ε'_r>180	ε''_r>36

the measurements. Since the acrylic thickness can be easily selected, the results of the uncertainty analysis need to be undertaken prior to actual measurements. On the other hand, although small surface imperfections need to be avoided, the effect of their influence can be evaluated after the measurements.

A. Uncertainty Analysis

For a few materials with permittivity within the representative range, the contribution resulting from the uncertainty in the scattering parameters was evaluated. After the initial complete analysis, it has been determined that, for nonmagnetic materials, lower total uncertainty is obtained if only S_{21}^* data are used. Therefore, uncertainty data presented use only S_{21}^* to obtain the permittivity.

Thicknesses of the sample, acrylic sample permittivity, and frequency all influence the uncertainty in a complex manner. A rigorous analysis needs to be performed that considers all parameters within their representative ranges. Only key results are illustrated. Fig. 3 shows the uncertainty in the dielectric constant and loss factor for a sample thickness in the 0.1–3-mm range and two acrylic thickness values. The complex permittivity was assigned a constant value ($\varepsilon'_r = 80$, $\varepsilon''_r = 10$) within the X-band, and represents a material of relatively low loss among the materials investigated. The curves are "thick" as they represent traces for multiple frequencies in the X-band. It is apparent that an acrylic thickness of 1 mm results in lower uncertainty compared with an acrylic thickness of 5 mm. Low uncertainty is attained at all frequencies for samples thicker than 1.5 mm. Reasonably low uncertainty for thicknesses 0.2–0.5 mm is also attained, which is of interest, as most samples are in this thickness range. For this specific material, sample thickness in the range of 0.8–1.3 mm is not desirable due to increased uncertainty of measurements.

Fig. 4 shows the uncertainty for two materials of higher loss factor, which are representative of radar absorbers. Due to the higher loss factor, the pseudoresonant effect at certain sample thicknesses (seen in Fig. 3) does not appear. There is only a relatively weak dependence of the uncertainty on frequency. Finally, even for very thin samples, of approximately 0.1–0.3 mm in thickness, low uncertainty is achievable for high dielectric constant and high-loss factor materials ($\varepsilon'_r = 100$, $\varepsilon''_r = 200$).

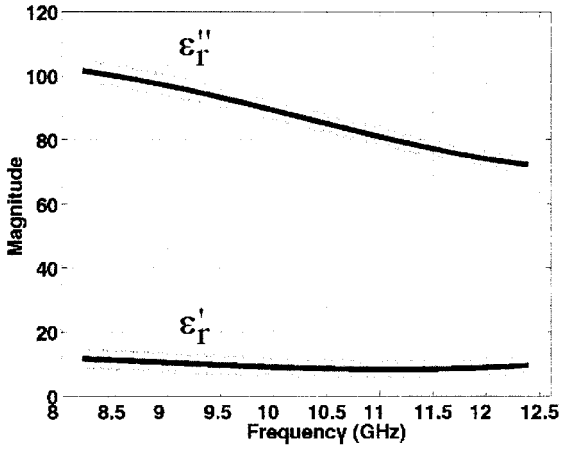

Fig. 7. Complex permittivity for a 0.15-mm-thick sample with acrylic thickness of 1.18 mm. Dashed lines indicate uncertainty limits of the permittivity resulting from S_{21} measurement.

Summary uncertainty plots are shown in Figs. 5 and 6 for several different ratios from ε'_r to ε''_r. These plots are helpful in determining expected uncertainty of a measurement.

Summary data from Figs. 5 and 6 are given in Tables I and II, where the acrylic thickness and frequency remain unchanged at 1 mm and 10 GHz, respectively. These tables provide ranges of material properties over which a desired uncertainty is achieved. For example, a value reads $\varepsilon'_r > 38$ in the "Uncertainty of ε'_r, <5%" column. This means that, in order for a measurement of a specific material, which has ratio of 0.5 from ε'_r to ε''_r, to be measured with an uncertainty of <5%, its electrical properties must be greater than $\varepsilon'_r = 38$ and $|\varepsilon''_r| = 19$.

It is clearly seen that lower (more desirable) numbers are, in general, found in Table II as the sample thickness is increased, but the dielectric constant and loss factor values in Table I are not extremely high, especially for the 1 : 1 ratio.

TABLE III
DIFFERENCES IN DIELECTRIC CONSTANT AND LOSS FACTOR FOR DIFFERENT CONFIGURATIONS OF FACIAL INCONSISTENCIES. ALL VALUES ARE AT 10 GHz

Condition	ε'_r	$\Delta\varepsilon'_r / \varepsilon'_r$	ε''_r	$\Delta\varepsilon''_r / \varepsilon''_r$
Perfect	**155.94**		**175.72**	
Gap #2	144.4	0.08	116.59	0.50
Gap #3	140	0.11	171.21	0.03
Gap #4	153.6	0.02	175.34	0.002
Dent #2	154.4	0.010	174.59	0.007
Dent #3	153.0	0.019	173.0	0.016
Dent #4	155.4	0.004	175.31	0.002

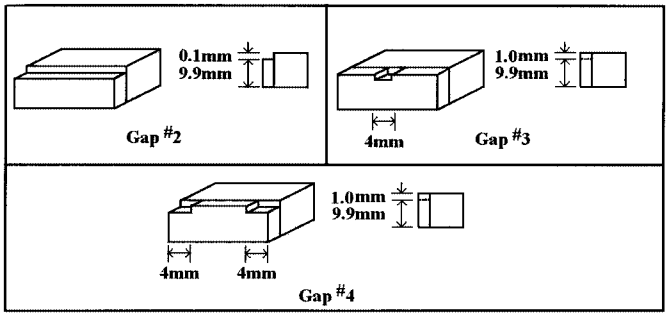

(a)

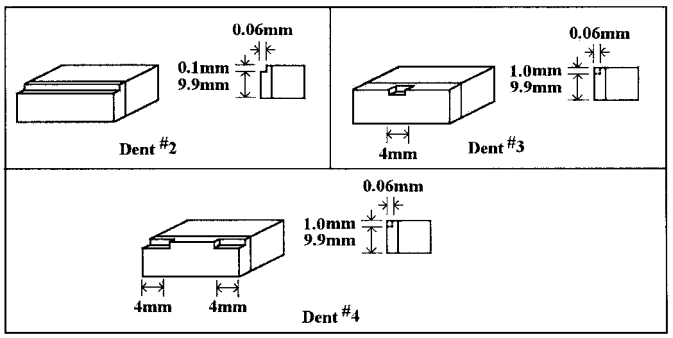

(b)

Fig. 8. Two-layer structure with imperfections in the TS, acrylic thickness 1.18 mm, and sample thickness 0.14 mm. (a) Gaps in sample. (b) Dents in sample surface.

B. Measurement Example

Fig. 7 presents experimental results for a typical TS. It has been evaluated with the uncertainty analysis that an increase in sample thickness to 1.5 mm would decrease the uncertainty of ε'_r from ∼30% to below 5%. Only a small improvement for ε''_r would be expected. In many circumstances, fabrication of a recommended sample thickness is not possible until a newer production process is developed.

Repeated measurements of the same sample invariably yielded very close results, well within the uncertainty limits. Similarly, for approximately 100 samples measured, whose properties ranged from ε' from 10 to 400, and ε'' from 5 to 800, results were obtained that fell within the uncertainty limits.

C. FDTD Modeling

A sample previously measured with the VNA having $\varepsilon'_r = 155.9$ and $\varepsilon''_r = 175.7$ at 10 GHz was simulated in the FDTD. The values of S_{21} were collected, and the electrical properties determined. Differences between the two data sets were less than 0.9% for both ε'_r and ε''_r. Table III shows data for this sample with the simulated facial inconsistencies of Fig. 8. These data indicate how the size and location of the sample imperfections influence the error in the measured permittivity. While small imperfections such as the dents considered here have only a small to moderate effect (1.9% for ε'_r, and 1.6% for ε''_r), full gap imperfections can effect the measured permittivity by as much as 50% (11% for ε'_r and 50% for ε''_r).

IV. CONCLUSIONS

A modified measurement method introduced for the characterization of permittivity of thin flexible high-loss materials has been shown to facilitate reasonably accurate measurements. A two-layer structure utilizing a supporting dielectric of known electrical properties is used. Since an explicit solution is not feasible for this configuration, an iterative algorithm is used to obtain material characteristics from the measured transmission coefficient. An uncertainty analysis presented facilitates finding the optimum thickness of the sample and supporting acrylic, and the FDTD modeling method quantifies the effect of small gaps and dents on the surface of the sample. The method described is suitable for measurements with uncertainty below 5% for 0.1-mm-thick samples with dielectric constant greater than 50 and a loss factor approximately equal to the dielectric constant. For 1-mm-thick samples a dielectric constant greater than six can be measured with uncertainty of less than 5% provided that the loss factor is roughly equal to the dielectric constant. Even higher accuracy can be obtained with a VNA of better accuracy than the model used in this analysis.

ACKNOWLEDGMENT

The authors gratefully acknowledge the contribution to the uncertainty analysis of D. Pasalic, Eidgenössische Technische Hochschule (ETH), Zurich, Switzerland (formerly of the University of Victoria, Victoria, BC, Canada).

REFERENCES

[1] G. W. Chantry, "The measurement of the properties of materials," *Proc. IEEE*, vol. 74, pp. 183–199, Jan. 1986.
[2] J. Baker-Jarvis, "Transmission/reflection and short-circuit line permittivity measurements," NIST, Boulder, CO, 1990.
[3] J. Baker-Jarvis, E. Vanzura, and W. Kissick, "Improved technique for determining complex permittivity with the transmission/reflection method," *IEEE Trans. Microwave Theory Tech.*, vol. 38, pp. 1096–1103, Aug. 1990.
[4] J. Baker-Jarvis, M. D. Janezic, J. H. Grosvenor, Jr., and R. G. Geyer, "Transmission/reflection and short-circuit line methods for measuring permittivity and permeability," NIST, Boulder, CO, Tech. Note 1355 (revised), Dec. 1993.
[5] J. Reinert, G. Busse, and A. F. Jacob, "Waveguide characterization of chiral material: Theory," *IEEE Trans. Microwave Theory Tech.*, vol. 47, pp. 290–296, Mar. 1999.
[6] G. Busse, J. Reinert, and A. F. Jacob, "Waveguide characterization of chiral material: Experiments," *IEEE Microwave Theory Tech.*, vol. 47, pp. 297–301, Mar. 1999.
[7] Z. Ma and S. Okamura, "Permittivity determination using amplitudes of transmission and reflection coefficients at microwave frequency," *IEEE Trans. Microwave Theory Tech.*, vol. 47, pp. 546–550, May 1999.
[8] E. Ni, "An uncertainty analysis for the measurement of intrinsic properties of materials by the combined transmission–reflection method," *IEEE Trans. Instrum. Meas.*, vol. 41, pp. 495–499, Aug. 1992.

[9] O. Tantot, M. Chatard-Moulin, and P. Guillon, "Measurement of complex permittivity and permeability and thickness of multilayered medium by an open-ended waveguide method," *IEEE Trans. Instrum. Meas.*, vol. 46, pp. 519–521, Apr. 1997.
[10] C. C. Courtney, "Time domain measurement of the electromagnetic properties of materials," *IEEE Trans. Microwave Theory Tech.*, vol. 46, pp. 517–522, May 1998.
[11] N. Belhadj-Tahar, A. Fourrier-Lamer, and H. de Chanterac, "Broadband simultaneous measurement of complex permittivity and permeability using a coaxial discontinuity," *IEEE Trans. Microwave Theory Tech.*, vol. 2, pp. 1–7, Jan. 1990.
[12] N. E. Belhadj-Tahar and A. Fourrier-Lamer, "Broadband simultaneous measurement of the complex permittivity tensor for uniaxial materials using a coaxial discontinuity," *IEEE Trans. Microwave Theory Tech.*, vol. 39, pp. 1718–1724, Oct. 1991.
[13] C. C. Courtney, "Time-domain measurement of the electromagnetic properties of materials," *IEEE Trans. Microwave Theory Tech.*, vol. 46, pp. 517–522, May 1998.
[14] C. C. Courtney and W. Motil, "One-port time-domain measurement of the approximate permittivity and permeability of materials," *IEEE Trans. Microwave Theory Tech.*, vol. 47, pp. 551–555, May 1999.
[15] P. A. Domich, J. Baker-Jarvis, and R. G. Geyer, "Optimization techniques for permittivity and permeability determination," *J. Res.*, vol. 96, no. 5, pp. 565–575, 1991.
[16] G. L. Friedsam and M. Biebl, "A broadband free-space dielectric properties measurement system at millimeter wavelengths," *IEEE Trans. Instrum. Meas.*, vol. 46, pp. 515–518, Apr. 1997.
[17] D. K. Ghodgaonkar, V. V. Varadan, and V. K. Varadan, "Free-space measurement of complex permittivity and complex permeability of magnetic materials at microwave frequencies," *IEEE Trans. Instrum. Meas.*, vol. 39, pp. 387–394, Apr. 1990.
[18] B. A. Munk, *Frequency Selective Surfaces*. New York: Wiley, 2000.

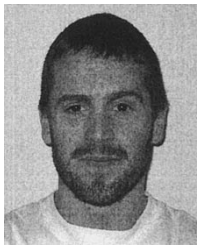

Trevor C. Williams (S'01) was born in Cranbrook, BC, Canada on July 18, 1975. He received the B.Eng. degree and Masters of Applied Science degree from the University of Victoria, Victoria, BC, Canada, in 2000 and 2002, respectively, and is currently working toward the Ph.D. degree in biomedical engineering at the University of Calgary, Calgary, AB, Canada.

His major field of study was microwave material measurement and radar absorber design. He is currently involved with tissue sensing adaptive radar for microwave breast imaging.

Maria A. Stuchly (S'71–SM'76–F'91) received the M.Sc. degree in electrical engineering from the Warsaw Technical University, Warsaw, Poland, in 1962, and the Ph.D. degree in electrical engineering from the Polish Academy of Sciences, Warsaw, Poland, in 1970.

From 1962 to 1970, she was with the Warsaw Technical University and the Polish Academy of Sciences. In 1970, she joined the University of Manitoba. In 1976, she joined the Bureau of Radiation and Medical Devices in Health and Welfare, Ottawa, ON, Canada, as a Research Scientist. In 1978, she was associated with the Electrical Engineering Department, University of Ottawa, as an Adjunct Professor. From 1990 to 1991, she was a Funding Director of the Institute of Medical Engineering. In 1992, she joined the University of Victoria, Victoria, BC, Canada, as a Visiting Professor with the Department of Electrical and Computer Engineering. Since January 1994, she has been a Professor and Industrial Research Chairholder funded by the National Sciences and Engineering Research Council of Canada, BC Hydro, and Trans Alta Utilities. Her current research interests are in numerical modeling of interaction of electromagnetic fields with the human body and wireless communication antennas.

Paul Saville, photograph and biography not available at time of publication.